International Global Navigation Satellite Systems Society
IGNSS Symposium 2006

Holiday Inn Surfers Paradise, Australia
17 – 21 July 2006

Paper Number: 15

Mitigation of Distance-Dependent Errors for GPS Network Positioning

Tajul A. Musa

School of Surveying & Spatial Information Systems
The University of New South Wales, NSW, Australia
Tel: +61-2-9313 4208 Fax: +61-2-9313 7493 Email: tajul.musa@student.unsw.edu.au

Samsung Lim, Thomas Yan, and Chris Rizos
School of Surveying & Spatial Information Systems
The University of New South Wales, NSW, Australia
Tel: +61-2-9313 4208 Fax: +61-2-9313 7493

ABSTRACT

The effect of the atmosphere has been identified as the major problem of long-baseline carrier phase positioning. The effect of the ionosphere, however, can be neutralised with dual-frequency observations. Thus, the effect of the troposphere is the challenge of precise positioning and needs to be mitigated in some way. The network-based approach provides a non-dispersive correction that can be useful in reducing this effect. Applying the correction to the ionosphere-free combination improves the ambiguity resolution and hence guarantees higher accuracy. In addition, dispersive and non-dispersive corrections can be separately applied to the computation of the receiver position.

KEYWORDS: GPS, Dispersive Effect, Non-Dispersive Effect, Network Corrections

1. INTRODUCTION

Long-baseline relative positioning is prone to distance-dependent errors: ***ionospheric effects, tropospheric effects and orbit errors***. Combined with station-dependent errors such as hardware-related errors, multipath, and measurement noises, they complicate the ambiguity resolution and impact on other parameters of interest. As a remedy, one may consider extending the observation session, applying a priori atmospheric modelling, utilising the dual-frequency relationship, implementing the precise orbit, etc. Without these options, fast and precise carrier phase positioning is only restricted to the short baseline case.

An electro-magnetic wave that propagates through the ionosphere is mainly affected by free electrons, quantified as the Total Electron Content (TEC). The ionosphere is a dispersive medium; that is, its refractive index is inversely proportional to the frequency. Fortunately, ionospheric effects on GPS observables are frequency dependent; so the corresponding time delay can be formulated and subsequently eliminated at least to the first order by observing multiple frequencies. The troposphere, however, is a non-dispersive medium; that is, the refractivity depends on meteorological conditions of the site and the atmospheric ray path. Thus, the time delay cannot be cancelled out by observing multi-frequency signals. Reducing the effect of the troposphere is very much reliant on an a priori model generated or predicted from previous observations. The same problem occurs with respect to orbital errors, which can be reduced by introducing precise orbit parameters rather than using the broadcast ephemeris, for example, predicted orbits from the International GNSS Service (IGS).

This paper discusses the effect of distance-dependent errors. Some theoretical aspects are assessed and real data are tested. It is evident from the analyses that more attention should be paid to the effect of the troposphere. Then, some background on the network-based approach is highlighted. In this study, the network-based correction is designed for handling the tropospheric delay by separating the dispersive and non-dispersive corrections from the network. Tests using a local network are presented.

2. DISTANCE-DEPENDENT ERRORS

2.1 Theoretical Background

In the following, simulations are conducted to highlight the effect of distance-dependent errors on GPS positioning. Based on 'mathematical' single-differenced (SD) observations and a geometrical analysis, Beutler et. al (1988) provides an excellent formulation to this problem. Here, the formulation has been tested to demonstrate the effect of distance-dependent errors.

a) Ionospheric effects on the baseline

For the carrier phase measurements, the effect of the ionosphere induces a scale error. Based on realistic TEC (measured in TEC units, or TECU), the mean vertical TEC (VTEC) is more likely to be in the range of 50 to 60TECU during periods of high solar activity, but can increase further to about 100TECU in the equatorial area.

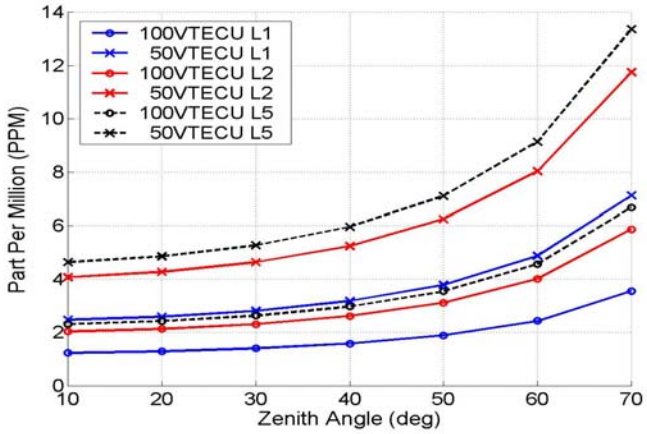

Figure 1. Baseline constraints due to the ionospheric delay at different zenith angles and VTEC values on L1 frequency; 1575.42MHz (blue), L2 frequency; 1227.60MHz (red), future L5 frequency; 1176.45MHz (dotted-black).

Figure 1 shows the simulation results assuming the VTECU value in the range of 50 to 100VTECU. The calculations vary with zenith angle and different VTECU on L1, L2 and future L5 frequencies. For the L1 frequency, maximum baselines are getting shorter due to the ionospheric delay, by between 7ppm and 3.5ppm depending on the satellite elevation at different TEC values. The effects are even higher for L2, which clearly indicates that the lower the frequency, the larger the error. The same can be expected for the future L5 GPS signals.

b) Tropospheric delay effect on the baseline

Considering two receivers located at the same altitude with identical meteorological conditions (i.e. temperature, pressure and humidity), the a priori tropospheric model (e.g. Saastamoinen model) should result in an identical correction. Thus, it can be assumed that both receivers have a 'common' tropospheric delay. Yet, both receivers view satellites at different zenith angles, which is dependent on the baseline length (receiver separation). The a priori tropospheric model is a function of the mapping function (i.e. zenith angle). The error introduced by neglecting this common tropospheric delay on the estimated baseline length is an absolute troposphere error. Now, consider two receivers located nearby (few km) but at different altitudes (e.g. a mountainous area vs. mean sea level), the meteorological conditions will be expected to be different at the stations. Any unmodelled error due to the effect of the troposphere, which cannot be handled by the a priori model at one receiver relative to the other, is referred to as a relative troposphere error. In this case, the effect of the relative troposphere error is more prominent because of the station height rather than the baseline length.

To simulate the effects of absolute and relative troposphere error, the unmodelled tropospheric delay is assumed to be in the range of 1cm to 10cm, for zenith angle from 0° to 70°. Figures 2 and 3 summarise the results. A few remarks can be made about the effect of tropospheric delay (absolute and relative):

a) Absolute troposphere error is distance-dependent; maximum effect of 10cm error at near horizon resulting in about 0.05ppm scale error for the estimated baseline.
b) Relative troposphere error is induced by station height differences; maximum effect at

near horizon is about three times the error, amplified by the mapping function.

c) Relative troposphere error is more serious than absolute troposphere error.

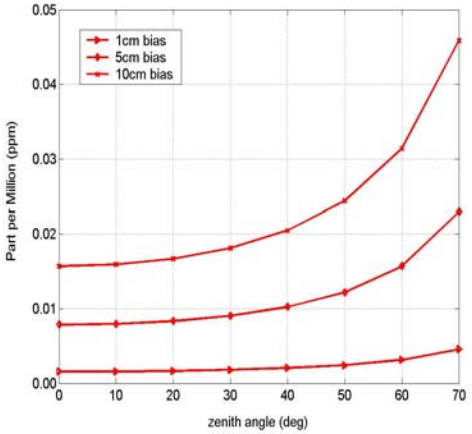

Figure 2. Error in baseline length (ppm) due to absolute troposphere error.

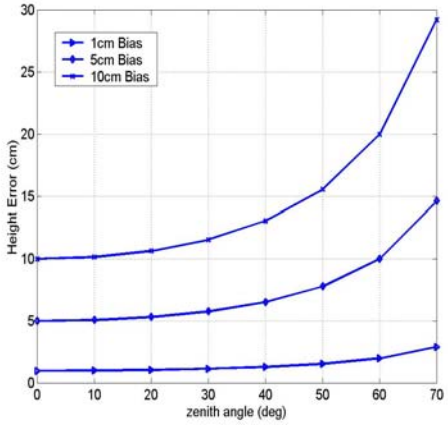

Figure 3. Error in station height (cm) due to relative troposphere error.

c) Orbital errors on baseline

Satellite orbital errors can be expressed in three orbit components: along-track, cross-track and radial error. The radial component is more likely to induce a larger effect compared to other components. The broadcast GPS orbits are much improved nowadays; with the accuracy typically better than 2m in RMS for all orbital components (IGS, 2005). Considering the RMS value is in the range 1-5m and the baseline length ranges from 100 - 500km, the baseline error is calculated and the results are summarised in Figure 4. The results show that the maximum orbital error of 5m produces only a 12.5cm error in the 500km baseline length (i.e., 0.25ppm). Hence, orbital errors are not serious if compared to the effect of the atmosphere.

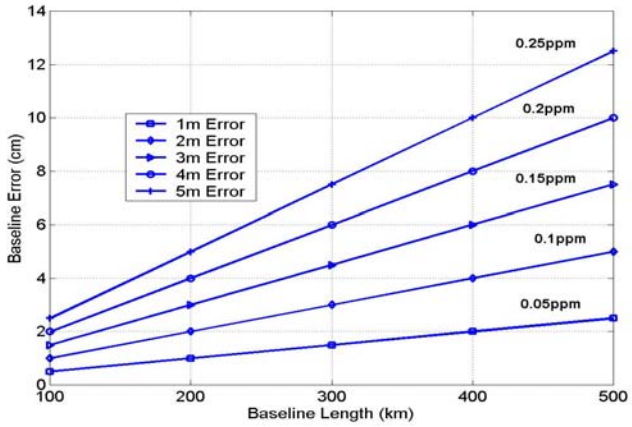

Figure 4 Baseline error (in cm) due to the effect of satellite orbital errors (m).

2.2 Residuals of Distance-Dependent Errors – The Equatorial Experiments

As the motivation of differencing is to 'eliminate' most common errors between the two receivers, the effectiveness is limited when dealing with long baselines due to distance-dependent errors. As a result, the residuals due to distance-dependent errors will remain. To highlight these residuals three different baseline lengths were selected. Sites are part of

Malaysian Active Surveying Stations (MASS) and the IGS global network in Singapore. They are located in the equatorial region, where severe effects of atmospheric delay can be observed.

The baselines were classified as short (UTMJ-NTUS, ~25km), medium-long (UTMJ-SEGA, ~143km) and long (UTMJ-BEHR, ~339km). The data were collected at Day of Year (DoY) 208/03 from 0:00 to 24:00UT/ 8:00am (27/7/03) to 8:00am (28/7/03) local time, at 30s epoch interval. The processing makes use of all options available (previously mentioned). It also takes advantage of the 'multipath-free' environment of permanent continuous operating reference stations (CORS), the known precise station coordinates, geodetic quality hardware and firmware, etc, in order to keep station-dependent errors at a minimum level. The BERNESE processing software has been employed (Rothacher & Mervart, 1996), and the double-differenced (DD) carrier phase ambiguities (i.e., L1, L2, widelane, narrowlane) were resolved where possible, and introduced for the analysis. All the data were masked at the 15° cut-off elevation angle.

a) Residuals ionospheric delay

The DD ionospheric delay residuals can be calculated from the analysis of the geometry-free measurements after introducing the L1 and L2 ambiguities from the previous run. Plots in Figure 5 show the DD ionospheric delay residuals (scale on L1) for all satellite combinations. The effect of the equatorial ionosphere becomes large between midnight and 4 o'clock local time. Large variations also occur after 14:00 local time, which points out that the behaviour of the equatorial ionosphere is indeed difficult to predict. As expected, the plots show that the long and medium-long baselines suffer from the ionospheric delay more than the short baseline. Obviously the residuals plots confirm that the ionospheric delay is distance-dependent.

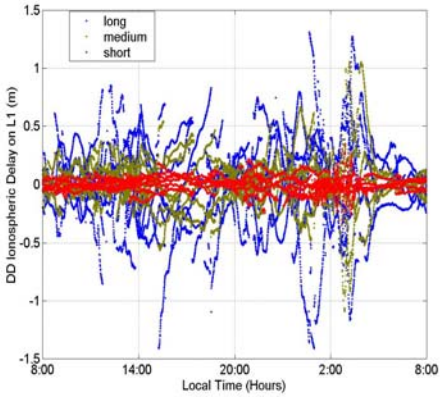

Figure 5. DD ionospheric delay residuals (scale on L1) for long, medium and short baselines.

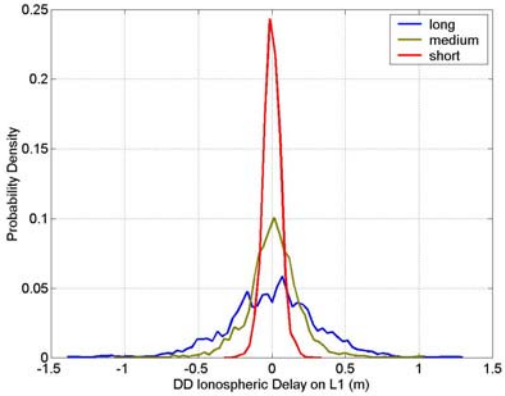

Figure 6. Statistical plots of residuals DD ionospheric delay for Figure 5.

Baseline	DD Ionospheric Delay on L1 (cm)			
	Min	Max	Mean	Stdv
Long	-141.83	131.21	0.06	32.98
Medium	-109.16	105.47	1.07	19.10
Short	-34.30	35.12	0.07	5.95

Table 1. Statistical analyses of DD ionospheric delay residuals for Figure 5.

Inspecting the statistical plots in Figure 6 and Table 1, the residuals reach over ±130cm for the long baseline, ± 100cm for the medium baseline, and ±30cm for the short baseline. This is equivalent to 6.3cycles, 5.3cycles and 1.6cycles of L1; 8.8cycles, 6.7cycles and 2.0 cycles of L2; 2.5cycles, 2cycles and 0.57cycles of widelane; for long, medium-long and short baselines respectively. This situation prevents from any success for 'direct' ambiguity resolution for L1, L2, or even widelane ambiguity resolution. The Ionosphere-Free (IF) combination and long observations spans are needed for successful ambiguity resolution during this time period. Despite that there are residuals smaller than 1 cycle (L1), but the probabilities are small and belong to a few satellite pairs at high elevation angle (even though this analysis is not provided here). In the case of the short baseline, the probabilities are higher compared to the others. However, the statistical results in Table 1 indicate the variations can reach up to 6cm. These conditions, plus other effects such as the tropospheric delay, orbital and station-dependent errors, easily complicate the direct ambiguity resolution. In practice, fast and (near) real-time ambiguity resolution is not possible for the above baselines, and is prone to failure even in case of a short baseline. If a single-frequency GPS receiver is to be used in this area (during this time), one needs to consider dealing with 'very short' baselines (must be much less than 25km) and an extended span of observations.

b) Residuals tropospheric delay

The IF is useful for approximating the tropospheric delay. Assuming station-dependent errors are at a minimum level with a sufficient baseline length or at a region where the tropospheric effect is quite severe, the DD IF residuals will be dominated by the tropospheric delay if DD IF ambiguity has to be resolved to its integer value. Figure 7 shows residuals of DD 'raw' tropospheric delay (i.e., no a priori troposphere is applied) derived from the DD IF combinations, which is obviously distant-dependent. The statistical analysis in Figure 8 and Table 2 further verify these results. The magnitude and variations of the residuals are less than, but almost similar to, the case of the ionospheric delay in the previous discussion. Therefore the same problem can be expected to arise from the residuals of the 'raw' DD tropospheric delay. The delay cannot be ignored and needs to be reduced to some extent.

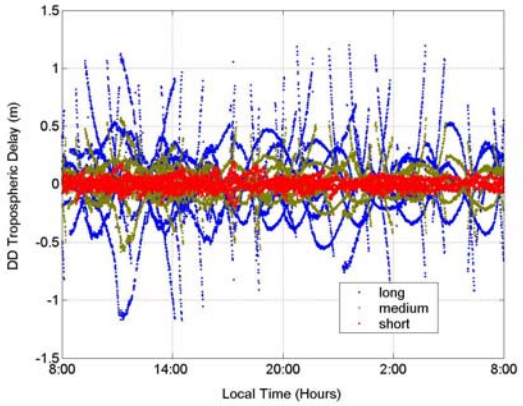

Figure 7. DD 'raw' tropospheric delay residuals (no a priori model applied) for long, medium and short baselines.

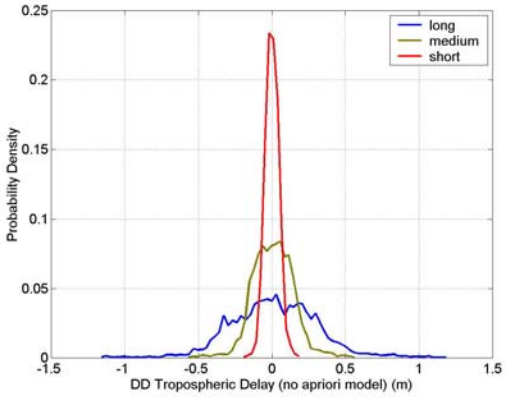

Figure 8. Statistical plots of the 'raw' DD tropospheric delay residuals for Figure 7.

Baseline	No A Priori Model (cm)			
	Min	Max	Mean	Stdv
Long	-117.16	119.98	1.81	30.53
Medium	-58.18	57.36	0.85	14.10
Short	-20.62	19.64	0.05	4.59

Table 2. Statistical analyses of 'raw' DD tropospheric delay residuals for Figure 7.

An a priori tropospheric model is often employed to reduce the delay. Plots in Figure 9 demonstrate the effectiveness of the a priori (total) Saastamoinen model in reducing the tropospheric delay. The noise from the IF combinations are evident from these plots. Variations of residuals for all baselines during the 24 hour processing are mostly 5cm, whereas the maximum and minimum values are about ±21cm. If the variations of 5cm could be used in Figure 3, it can be expected that the station height errors during the test will reach 15cm for low elevation satellites.

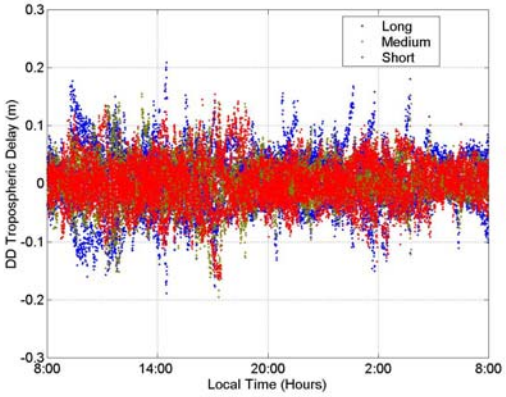

Figure 9. DD tropospheric delay residuals after applying the Saastamoinen model for long, medium and short baselines.

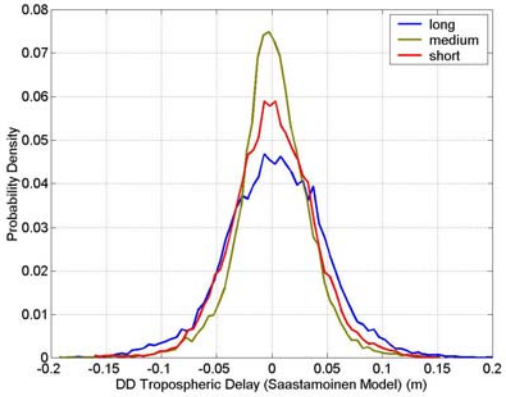

Figure 10. Statistical plots of DD tropospheric delay residuals for Figure 9.

Baseline	Saastamoinen Model (cm)			
	Min	Max	Mean	Stdv
Long	-18.84	20.90	0.35	4.54
Medium	-19.53	15.49	0.10	3.29
Short	-16.32	15.43	0.07	3.66

Table 3. Statistical analyses of DD tropospheric delay residuals for Figure 9.

Interestingly, the residuals for the short baseline do not improve much compared to the others. Moreover, the distance dependency is not obvious. Checking the station coordinates, the height difference (ellipsoidal height is enough for this purpose) between UTMJ-NTUS is only ~1 metre. Thus, the height difference is not likely to be the factor that explains this result. The explanation could be the difference of meteorological conditions between the two sites during the observations. This is not rare for Tropical Rainforest areas where large magnitude and short-term variations of wet delay (mostly due to water vapour in the atmosphere) can be observed. In addition, the site NTUS in Singapore is exposed to the ocean. If this is the case, it also highlights another difficulty in handling the residuals of the DD tropospheric delay. The delay is distance-dependent and is very much influenced by the site's meteorological conditions due to their different altitude, but is also affected by weather conditions which are significantly different at the two sites. Unfortunately, the meteorological information is often

limited.

d) Residuals orbital errors

The residual from DD orbit errors can be studied by subtracting the geometric range of the observations between the broadcast or ultra-rapid orbit (from IGS). In this study, the DD IF is employed using the aforementioned procedure. Plots in Figure 11 show that the residual of the DD orbit errors are distance-dependent. In the case of the broadcast orbit, it can be noted that there are large variations during the period 14:00-20:00 (6:00-12:00UT) for the long and medium baselines. Maximum and minimum residuals in Table 4 reach above ±10cm for the long baseline, and less than ±6cm for the medium-long baseline. The trends also show large residuals repeated at around 2-3am local time. It is not clear what the cause of these variations is. One of the explanations could be that the broadcast orbit uploads a new message during this time, when the old orbit becomes less reliable (note that the GPS Master Control Station uploads messages at around 2am local time). Raquet (1998) found a similar problem when analysing a baseline (~460km in length) in the southern part of Norway. In the case of the short baseline, the residuals are less prominent. The variations during the 24 hour test are less than 1cm.

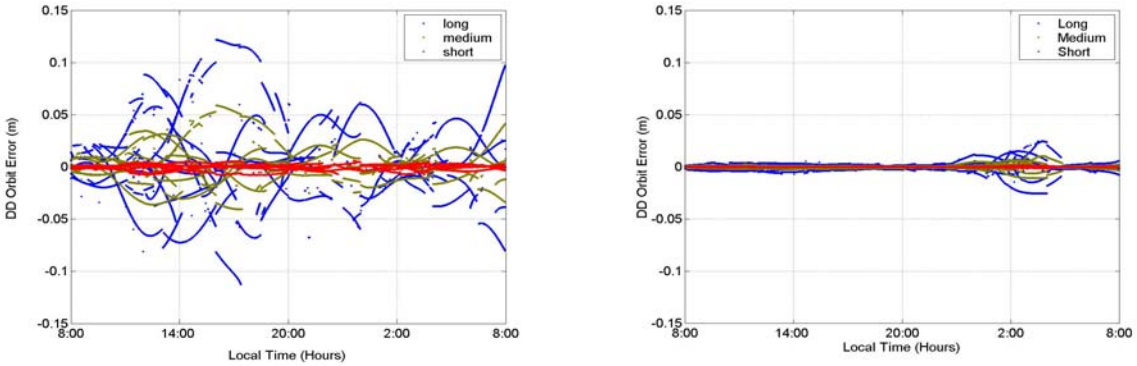

Figure 11. Residuals of the DD orbital errors; broadcast minus precise orbit (left); ultra-rapid minus precise orbit (right); for long, medium and short baselines.

For the ultra-rapid orbit, the plot clearly shows that the residuals are too small, with variations less than 1cm for the long baseline. Some variations can be detected for the period 23:00-4:00 local time. Similar to the broadcast orbit, these large variations could be caused by less precise satellite position at the end of the prediction time. For real-time applications, the ultra-rapid orbit from the IGS is the better option. Clearly from this discussion, the orbital errors are not that serious when compared to the atmospheric delay, which reflects the theoretical assessment in Section 2.1(c).

Baseline	**Broadcast - Precise Orbit (cm)**				**Ultra - Precise Orbit (cm)**			
	Min	Max	Mean	Stdv	Min	Max	Mean	Stdv
Long	-11.26	12.19	0.29	3.70	-2.56	2.49	0.01	0.51
Medium	-4.06	5.91	0.15	1.63	-1.07	1.11	0.00	0.23
Short	-0.79	0.71	0.03	0.27	-0.12	0.15	0.00	0.03

Table 4. Statistical analyses of DD residuals orbital errors for Figure 11.

3. THE NETWORK-BASED APPROACH

The concept and technique of differential, carrier phase network-based positioning was introduced by Wanninger (1995), utilising at least three reference stations from a local GPS CORS network. The technique allows users to better estimate the effect of distance-dependent errors in the surrounding area. The estimated errors can be geometrically modelled to support user positioning activities within the network coverage. Interestingly, the technique also allows implementation in the real-time kinematic (RTK) mode. Figure 12 illustrates the basic concept of the technique. In general, the technique requires all GPS reference stations to transmit their measurements to a control centre. The network algorithm at the control centre will select one of them as a master station, then calculate and distribute the network corrections to all users. This process is described as a series of steps in Figure 13.

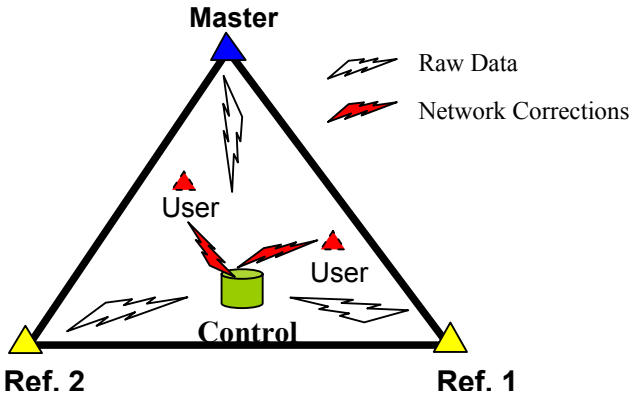

Fig. 12. Basic concept of network-based RTK.

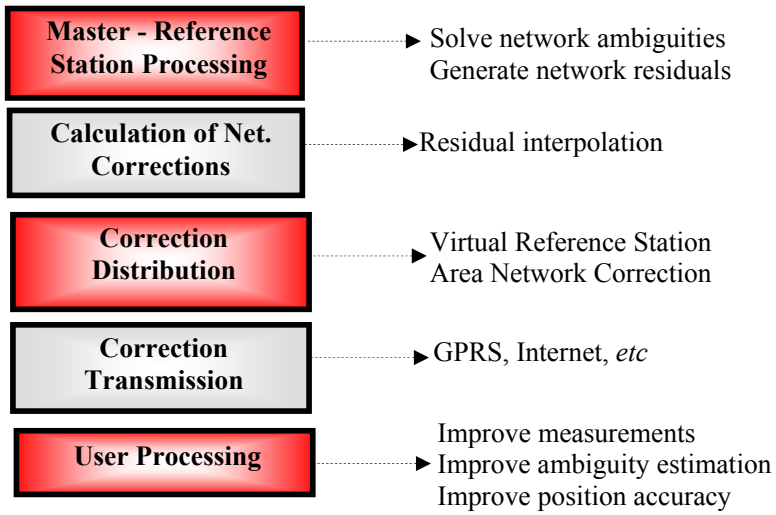

Figure 13. Network-based RTK processing steps.

For the master-reference station processing, the main objective is to resolve the network ambiguities (between the master and other reference stations). Once the network ambiguities are "fixed" (or resolved to their correct integer value), the residuals are used to approximate distance-dependent errors within the area (while assuming station-dependent errors are at a minimum). The use of fixed network residuals will ensure that high-quality network corrections can be generated through the interpolation process. A linear interpolation

algorithm is adequate to perform this task for a local network. Dai (2002) has discussed different interpolation methods that can be used for this purpose. The network corrections, containing information about the distance-dependent errors, need to be distributed to users. Currently, in real-time mode, two distribution options are popular: Virtual Reference Station (VRS) (Lynn & Anil, 1995; Wanninger, 1997), and Area Correction Parameter (FKP) (Wubbena & Bagge, 1998). Advantages and disadvantages of the two techniques can be found in Landau *et. al* (2003). The next step is to transmit the network corrections to users via various media such as internet, radio modems, *etc*. Any transmission delay needs to be addressed properly, which is beyond the scope of this paper. Finally, the corrections can be applied to users' measurements so as to improve the ambiguity resolution process and ultimately the positioning results.

3.1 Dispersive & Non-Dispersive Approach

Since the processing centre has a capability to isolate dispersive (ionosphere related) and non-dispersive (troposphere related) effects, this property is advantageous to the network users in many ways. Here the focus is to assist ambiguity resolution from master station to user station when using the IF combination. It is not possible to directly solve the DD IF because of the short wavelength of ~6mm. The following approaches for master to user station ambiguity resolution are proposed:

Step 1: Estimate the widelane ambiguity (with a combination of the narrowlane code-range or phase-range only).
Step 2: Improve IF combination with non-dispersive correction; on an epoch-by-epoch, satellite-by-satellite basis.
Step 3: Estimate the L1 ambiguity via the IF combination, along with the fixed widelane ambiguity.
Step 4: Ambiguity search, decorrelation and validation.
Step 5: Adaptation.

Step 1: Some advantages of the widelane plus code narrowlane combinations are: (1) it is geometry-free (GF) and IF, and therefore independent on the baseline length, (2) it has a longer wavelength of ~86.2cm, and, most important of all, (3) the widelane ambiguity at each epoch for each satellite can be estimated. Typically, multipath in the pseudo-ranges reduces the quality of the estimated ambiguity because of its long wavelength (30m). Since the beginning of operation or a new satellite signal is acquired, a sequential approach is implemented to smooth the pseudo-ranges and enhance the estimated widelane ambiguity. In case of loss-of-lock, the process needs to be restarted as the integer clearly 'jumps' to a new value. In low multipath environments, plus if hardware and firmware can reject multipath, and if the widelane measurement residuals are less than a half of its wavelength, real-time ambiguity resolution is possible simply by rounding-off to the nearest integer value. Another approach is to use the classical widelane (phase only), however the combination is contaminated by the atmospheric effects that need to be reduced, for example, by using IGS global ionospheric estimation.

Step 2: It is assumed that network users receive raw measurements of the master station plus the non-dispersive correction. Cancelling the ionospheric delay is the main reason why the IF combination is used. Since the IF combination is dominated by the tropospheric delay (Section 2), the non-dispersive correction generated by the processing centre improves the IF combination. Using the IGS ultra-rapid orbit also reduces the orbital errors. Measurements

noise should be handled with stochastic modelling. A further assumption is that the quality of the raw measurements can be characterised by a simple stochastic model.

Step 3: Despite its short wavelength, the IF combination preserves the integer ambiguity. Thus, it is useful to estimate L1 and L2 ambiguity independently when the widelane ambiguity in Step 1 is fixed (Blewitt, 1989). In view of the fact that the wavelength of L1 via the IF combination is only 10.7cm. Thus, to apply the non-dispersive correction and better orbit information is a clear advantage in this step.

Step 4: Least squares ambiguity decorrelation adjustment (LAMBDA) (Teunissen, 1994) is introduced for the ambiguity search and decorrelation. Additionally, the ambiguity validation procedure and the F-ratio test (Frei and Buetler, 1990) can be used to validate the ambiguity estimates. The process evaluates the ratio based on probabilistic properties of the best and the second best ambiguity residuals against a critical value. This statistical process has its own problems, and these are discussed in Verhagen (2004). For this reason, Step 5 is included.

Step 5: This procedure removes some low elevation satellites (and repeats Step 4) when the ambiguity validation fails. If the validation check is passed, a check is performed on the 'fixed' residuals against a 'threshold' value. The value can take the difference between the DD ionospheric delay scale on L1 and L2, which is set less than 5cm (Han, 1997). The rationale behind this is that measurements with large residuals may have wrong ambiguities. Measurements beyond this threshold should be rejected. Hence, Step 4 can improve the reliability of the fixed ambiguities. If real-time ambiguity validation still fails, 'near' real-time ambiguity resolution should proceed through a sequential approach.

Once the ambiguity resolution is completed, the fixed L1 and/or L2 ambiguity should be removed from the original measurements before performing the user's position computation. The positioning accuracy is now dependent on the satellite geometry and the station-/distance-dependent residuals. The distance-dependent errors are dominant in that they are still present in the fixed measurements. Both dispersive and non-dispersive corrections are now applied to each epoch and each satellite with an expectation that it reduces the distance-dependent errors in the users' position computation. It is worth mentioning that the same algorithm is used to generate the network corrections (i.e., dispersive and non dispersive) from master to other reference stations, except no network correction was applied. As reference stations, it also takes advantage of long hour observations in resolving the master-to-reference ambiguities and calculates the corrections beforehand. The network corrections were generated on an epoch-by-epoch, satellite-by-satellite basis, assuming the distance-dependent errors exhibit linear behaviour. The linear combination method was applied in the interpolation process (Han, 1997).

4. THE EXPERIMENTS

A small network known as Singapore Integrated Multiple Reference Station Network (SIMRSN) located near the equator (latitudes 1° 15' – 1° 30'N, and longitudes 103° 40' – 103° 59'E) was used in this experiment. It is expected that atmospheric effects were severe on this island and are sufficient to test the proposed strategy. Figure 14 shows the locations of the SIMRSN stations. Station LOYA is selected as the master station, while station NYPC is treated as a user station. The selection is made to avoid severe multipath for the user station because the proposed network algorithm is not intended to mitigate such effects at this stage. Other stations were considered to be reference stations. The test was conducted on DoY

166/03, and the observations period was 2hrs 50minutes (start at 8.00 am local time) with 15s epoch data.

The network correction (i.e. dispersive and non-dispersive terms) was first generated by removing satellites in the master-to-reference combinations whose elevations were less than 10°. Figures 15 and 16 show the DD ionospheric delay (on L1) and DD tropospheric delay with the corresponding dispersive and non-dispersive corrections for master-to-user station. For the non-dispersive correction, an averaging function can be applied for up to few epochs. This is reasonable since the variation of the tropospheric delay is less regular than that of the ionospheric delay.

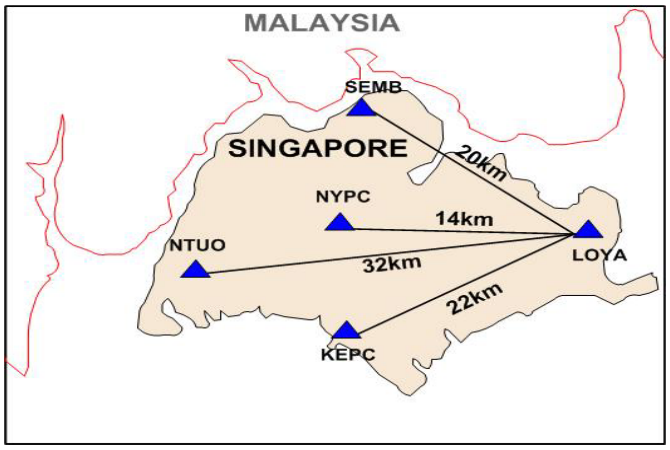

Figure 14. SIMRSN stations.

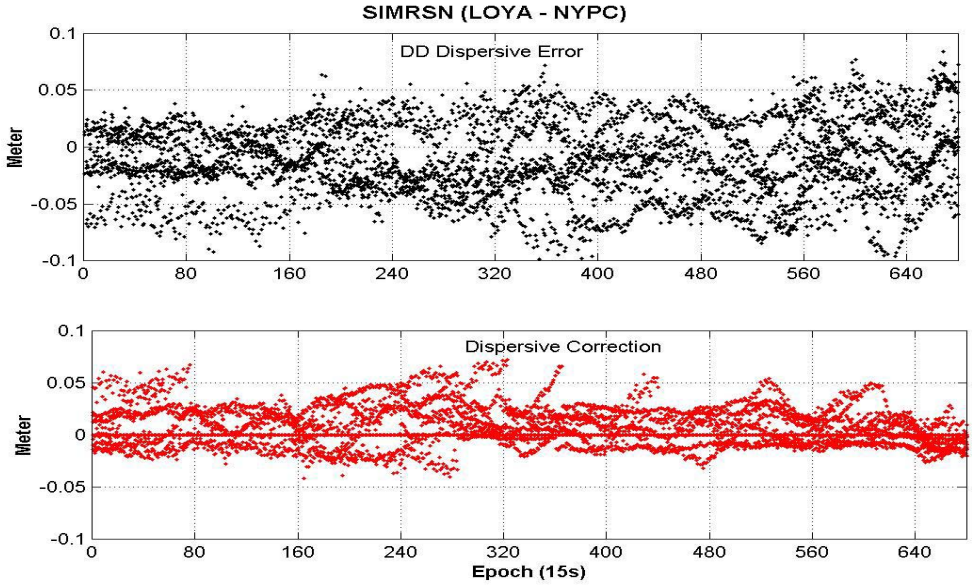

Figure 15 DD ionospheric delay (dispersive effect) for all satellite combination and the corresponding dispersive correction (note the line at zero value indicate no correction exists for some particular satellites) for LOYA-NYPC (master-user-station).

To investigate the proposed network processing strategy, tests were conducted in post-processed mode, although they 'simulated' the RTK mode. For verification purposes, the data

has been processed in static mode, where the most probable ambiguities were set as 'known' values. In comparison, a single-base technique i.e. master-to-user station has been processed using the aforementioned procedure but without any network correction. Therefore, a direct comparison can be made since both processing procedures only differ from with- and without the network corrections.

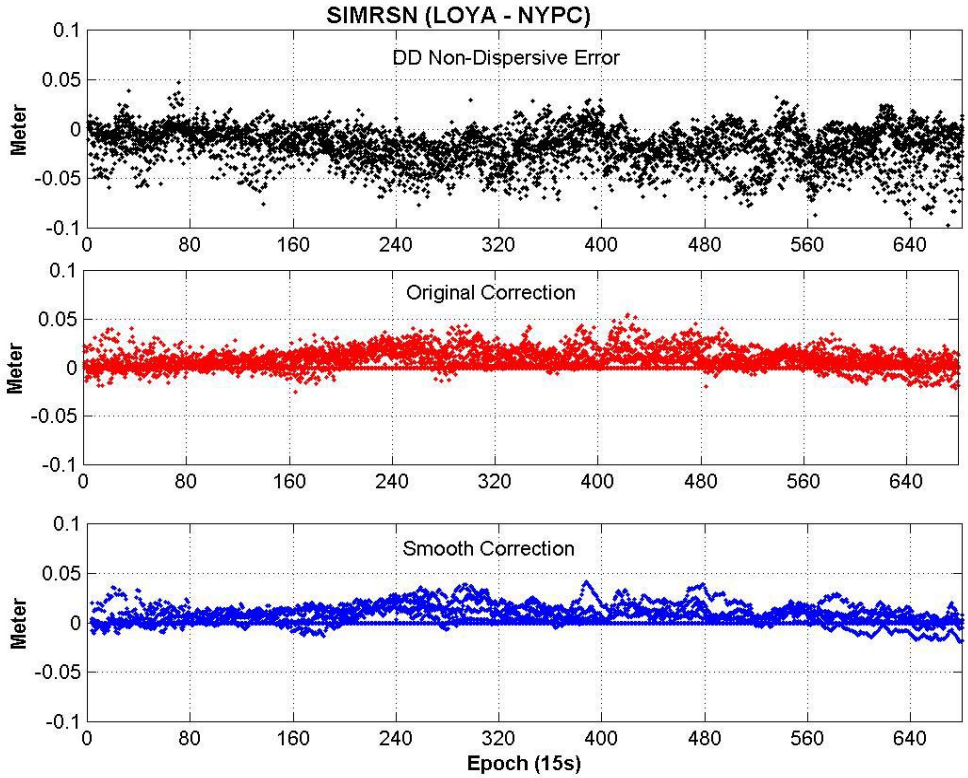

Figure 16 Up: DD non-dispersive error; Middle: original non-dispersive correction; Bottom: smoothed correction; for all satellite combinations. Note that some corrections are not available indicated by a line at zero value.

Table 5 shows the ambiguity resolution result from single-base and network-based techniques. It can be noted from the Table that the network-based technique provides better results for correct, rejected and wrong ambiguity when compared to the single reference DGPS mode. Figure 17 show the residuals of DD 'fixed' L1 observation for both techniques. The residuals for the network-based technique on average are improved since the dispersive and non-dispersive corrections are applied to the fixed measurements.

Cut-off Elevation	Case Initialize	Single Reference			Network-Based		
		Correct %	Reject %	Wrong %	Correct %	Reject %	Wrong %
10°	4665	96.4	2.1	1.5	98.7	0.8	0.5
15°	3584	97.4	2.4	0.2	99.3	0.7	0
20°	3033	98.5	1.4	0.2	99.6	0.4	0

Table 5. Statistics of ambiguity validation for SIMRSN compared to known ambiguities.

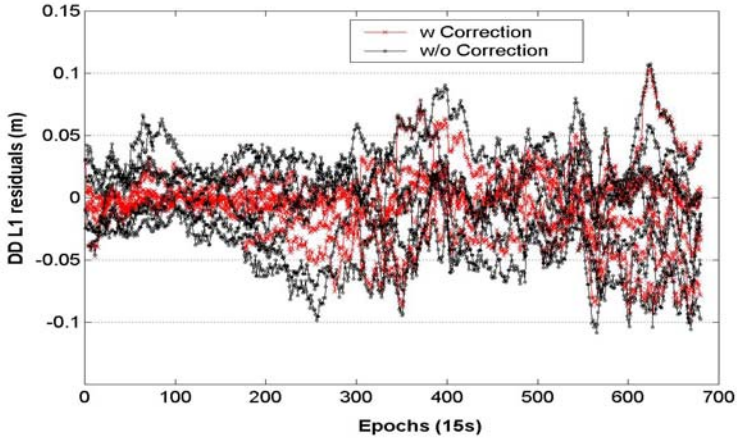

Figure 17. Fixed DD L1 residuals for all satellite combinations from the single-base (black) and network-based techniques (red).

Table 6 summarises the statistics of the coordinate differences between the known coordinates (from the network provider) and the estimates from both techniques at each epoch. From the Table an improvement of the mean Up component can be obtained once the corrections are applied. This results from the non-dispersive correction which reduces the residual tropospheric biases in the measurements. There are no significant differences found in the North component, but some improvements to the East component of NYPC are noticed. The variations of the Up component also show some improvements at 15° and 20° cut-off elevation for the network-based technique.

Cut-off Elev.	Corr	Mean (cm)			Stdv (cm)		
		dE	dN	dUp	dE	dN	dUp
10°	w/o	-4.7	0.5	-5.1	1.0	1.0	2.8
	With	-2.4	0.4	-2.8	1.3	0.7	2.8
15°	w/o	-4.5	0.4	-4.4	1.5	1.1	3.5
	With	-2.1	0.5	-1.8	1.8	0.8	2.5
20°	w/o	-4.1	0.4	-5.4	1.5	1.5	5.9
	With	-1.8	0.5	-1.8	1.7	0.9	3.2

Table 6. Position statistics for NYPC with and without (w/o) corrections; the difference with respect to known position of NYPC.

5. CONCLUDING REMARKS

Long-range carrier phase relative positioning is influenced by distance-dependent errors. The largest effect comes from the ionosphere and it limits the baseline length, though it can be effectively eliminated by dual-frequency observations. Orbital errors have similar affects but are smaller in magnitude; the effect can be reduced by using better orbits. Thus, the most problematic error is the tropospheric delay. Distance-dependent errors create a problem for fast carrier phase ambiguity resolution. They limit the baseline length to some extent, and generally, must be in the range so that differencing process removes the error. Analysis of residuals of distance-dependent errors in the equatorial region shows that the effective range must be much less than 25km.

The network-based positioning technique allows for the modelling of distance-dependent errors. One of the advantages is that the modelling can isolate the dispersive (ionosphere related) and non-dispersive (troposphere related) effects at the residual analysis. Hence, the non-dispersive correction is useful for reducing the effect of the troposphere, which dominates the IF combination. Such improvement is important, especially for indirect ambiguity resolution via IF combination. Experiments over a small network in a region of severe atmospheric delay demonstrate that the proposed approach improves both ambiguity resolution and positioning results. In fact, there is no reason why the baseline length cannot be extended further than the one used in this study. In practice, the impact of station-dependent errors could limit this approach when implemented in the real-time mode.

ACKNOWLEDGEMENTS

The authors would like to thank the administrators of MASS, SIMRSN and IGS for providing the data in this study.

REFERENCES

Beutler G, Bauersima I, Gurtner W, Rothacher M, Schildknecht T, Geiger A (1988) Atmospheric refraction and other important biases in GPS carrier phase observation, Monograph 12, School of Surveying, University of New South Wales, Sydney

Blewitt G (1989) Carrier phase ambiguity resolution for the Global Positioning System applied to geodetic baselines up to 2000km, *Journal of Geophysical Research*, 94(B8): 10187-10203

Dai L (2002) Augmentation of GPS with GLONASS and pseudolite signals for carrier phase-based kinematic positioning. PhD Thesis, School of Surveying and Spatial Information Systems, The University of New South Wales, Sydney

Frei E, Beutler G (1990) Rapid static positioning based on the fast ambiguity resolution approach FARA : theory and first results, *Manuscripta Geodaetica*, 15 (4): 325-356

Han S (1997) Carrier phase-based long-range GPS kinematic positioning, *PhD Thesis*, School of Surveying and Spatial Information Systems, The University of New South Wales, Sydney

IGS (2005) International GNSS Service, IGS Central Bureau, Pasadena, via (http://igscb.jpl.nasa.gov)

Landau H, Vollath U, Chen X (2003) Virtual reference stations versus broadcast solutions in network RTK – advantages and limitations, *Proceedings of GNSS2003*, The European Navigation Conference, Graz, (CD-ROM proceedings)

Lynn W, Anil T (1995) DGPS architecture based on separating error components, virtual reference stations and FM sub-carrier broadcast, *Proceeding of ION AM-1995*, Colorado Springs, 128-139

Raquet JF (1998) Development of a method for kinematic GPS carrier-phase ambiguity resolution using multiple reference receivers, *PhD Thesis*, Dept. of Geomatic Eng., The University of Calgary, Alberta

Rothacher M, Mervart L (1996) Manual of Bernese GPS software, version 4.0, Astronomical Institute, University of Berne, Berne

Teunissen PJG (1994) A new method for fast carrier phase ambiguity estimation, *Proceedings of IEEE PLANS 1994*, Las Vegas, 562-573

Verhagen S (2004) Integer ambiguity validation: an open problem? *GPS Solution*, 8(1): 36-43

Wanninger L (1995) Improved ambiguity resolution by regional differential modeling of the ionosphere, *Proceedings of ION GPS-1995*, Palm Springs, 55-62

Wanninger L (1997) Real-time differential GPS error modeling in regional reference station networks, *Proceedings of IAG Symp 118*, Rio de Janeiro, 86-92

Wübbena G, Bagge A (1998) GNSS multi-station adjustment for permanent deformation analysis networks, *Proceedings of the Int. Symp. on Geodesy for Geotechnical & Structural Engineering*, Eisenstadt, 139-144